JOURNAL OF THERMOPHYSICS AND HEAT TRANSFER
Vol. 7, No. 2, April–June 1993

Thermal Conductivities of Quantum Well Structures

G. Chen* and C. L. Tien†
University of California, Berkeley, Berkeley, California 94720

This work analyzes the size and the boundary effects of a gallium arsenide- (GaAs) based quantum well (QW) structure on the thermal conductivity of the well material. Calculations show that the order of phonon mean free path (MFP) is equal to or even longer than the typical dimension of the well (~200 Å or less). Holland's model is applied to match the thermal conductivity data of bulk GaAs from 2 to above 600 K. The equation of phonon radiative transfer (EPRT) developed from the Boltzmann transport equation is then introduced for the heat transport in the QW structure. Boundary conditions are built from the diffuse phonon mismatch theory, and approximate solutions are obtained for the cases of heat flow perpendicular and parallel to the well. Results show that the thermal conductivity of the quantum well can be one order-of-magnitude lower than that of its corresponding bulk form at room temperature. The size and boundary effects also cause anisotropy of the thermal conductivity, even though the unit cell of GaAs is cubic.

Nomenclature

a = lattice constant
C = constant, C_i, $\kappa^4/(2\pi^2\hbar^3 v_i)$
c = volumetric specific heat
D = density of state
E = exponential function
F = boundary scattering correction factor
f = phonon distribution function
G = constant
g = universal function
h = film thickness
$\hbar$ = Planck constant divided by 2π
I = phonon intensity
k = thermal conductivity
L = characteristic length of crystal
M = atomic mass
N = total number of primitive cells
p = fraction of specular phonon reflection
q = heat flux
R = quantity given by Eq. (28)
T = temperature
V = crystal volume
v = phonon group velocity
x = $\hbar\omega/\kappa T$, or AlAs concentration
y = coordinate parallel to film
z = coordinate perpendicular to film
α = coefficient, or transmission coefficient
β = coefficient
γ = Euler constant
ζ = nondimensional distance, $z/\tau_i v$
η = mean square root deviation of surface roughness
θ = angle in Fig. 1, temperature
κ = Boltzmann constant
Λ = phonon MFP
λ = phonon wavelength
$\boldsymbol{\lambda}$ = vector in displaced Planck distribution
μ = $\cos\theta$
τ = relaxation time
φ = angle in Fig. 1b
Ψ = universal function
Ω = solid angle
ω = angular frequency

Subscripts
b = boundary
D = at Debye temperature
h = at $z = h$
i = internal scattering or medium i
3-i = medium adjacent to medium i
j = phonon polarization
L = longitudinal phonon
n = normal process
q = phonon wavevector
t = total quantity
to = transverse phonon at low frequency
tu = transverse phonon in umklapp process
u = umklapp process
y = y component
z = z component
ω = spectral quantity

Superscripts
0 = at equilibrium
+ = positive direction, $0 < \theta < \pi/2$
− = negative direction, $\pi/2 < \theta < \pi$

Introduction

GALLIUM arsenide- (GaAs) based quantum well (QW) structures represent a rapidly expanding area of research and development. A quantum well structure often consists of one or more ultrathin (~200 Å or less) low bandgap semiconducting layers, embedded in a high bandgap medium. Electrons in such ultrathin layers (the active region) display strong quantum size effects due to the difference in the bandgap energies of the confining and well materials, which greatly change the electrical and optical properties of the structure. Devices based on QW often have superior characteristics. For example, QW semiconducting lasers have much lower lasing threshold currents and are becoming the key elements in optical fiber communication and optical storage.[1] They can also act as electronic-to-optical and optical-to-electronic interfaces, which make the integration of optics and electronics possible.

Thermal conductivity is an important parameter in the design of the power consumption devices. For GaAs-based QW lasers, it affects their operating temperature, stability, output mode, and packing density. One problem in the design of better semiconducting lasers is heat dissipation. Several existing thermal models use bulk thermal conductivity data in

Presented as Paper 92-0707 at the AIAA 30th Aerospace Sciences Meeting, Reno, NV, Jan. 6–9, 1992; received Jan. 17, 1992; revision received April 28, 1992; accepted for publication April 28, 1992.

*Graduate Student Researcher, Department of Mechanical Engineering.
†A. Martin Berlin Professor of Mechanical Engineering. Fellow AIAA.

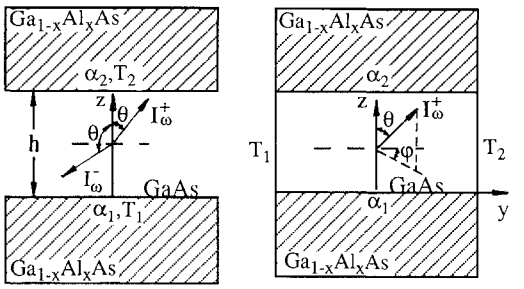

Fig. 1 Sketch of a quantum well and the coordinate systems: a) heat flow perpendicular to the well, b) heat flow parallel to the well.

their calculations.[2] However, due to the small dimension of QW structures, the validity of the bulk thermal conductivity is subject to question.

Study of size effects on thermal conductivity originated from the experimental work of de Haas and Biermasz[3] and the theoretical explanation by Casimir.[4] Both Casimir and later Berman et al.[5] considered the very low temperature limit and used the photon radiation heat transfer analogy, because at very low temperatures all other scattering mechanisms inside the specimen are suppressed, therefore, only boundary scattering is important. Similar results were also obtained by Ziman[6] from the Boltzmann transport equation (BTE). At higher temperature, when both the internal and the boundary scattering effects are important, Matthiessen's rule[6] is often applied to obtain the total phonon relaxation time, though its validity for the boundary scattering has never been vigorously proven. Herring[7] and Carruthers,[8] however, started from the BTE and obtained an equivalent boundary scattering relaxation time so that Matthiessen's rule is valid in form.

Recent measurements on thin films of micron range show that their thermal conductivities are generally much lower (e.g., 1–2 orders-of-magnitude), than those of their corresponding bulk materials.[9] Some plausible explanations include the columnar structure, cracks, and porosity produced during the formation of the films. Redondo and Beery[10] developed a microcrack model to explain the reduction of the thermal conductivity. Volklein and Kessler[11] concluded that both the boundary scattering and the columnar structure should be included in explaining the thermal conductivity of polycrystalline bismuth films. Flik and Tien[12] used a simple geometric argument and obtained the phonon mean free path (MFP) reduction for superconducting thin films.

In a GaAs QW structure, the active region is sandwiched between $Ga_{1-x}Al_xAs$ alloys, as shown in Fig. 1. Most heat flows perpendicularly through the layer and the confining media to the substrate. In this case, the transmission and reflection of phonons at the solid interfaces as well as the finite film thickness should be considered. An example of the effects of phonon transmission and reflection at an interface is the thermal boundary resistance.[13]

This article conducts a theoretical study of the size and boundary effects of the active region on its thermal conductivity. Holland's model is used to match the thermal conductivity data of bulk GaAs from 2 to 600 K. In a QW, the equation of phonon radiative transfer (EPRT)[14] developed from the BTE is applied. Boundary conditions are incorporated to obtain the thermal conductivity in the direction perpendicular as well as parallel to the film. The results show that the thermal conductivity of the well material can be much lower than that of its corresponding bulk form, even at room temperature. Anisotropy of thermal conductivity caused by the size and boundary effects is also presented.

Phonon MFP

The thermal conductivity of a gas from classical kinetic theory is[15]

$$k \approx cv\Lambda/3 \tag{1}$$

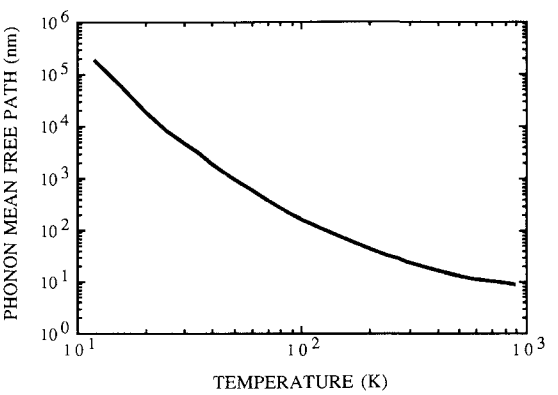

Fig. 2 Phonon MFP as a function of temperature for GaAs.

By analogy, phonons can be treated as a phonon gas, and the above formula can be used as a definition for the phonon MFP Λ.[6,8] Although the theoretical calculation of Λ is not easy, the above formula can serve as an estimation of Λ if other quantities are known through experiment.

Figure 2 shows the phonon MFP variation of bulk GaAs with temperature calculated from Eq. (1). Thermal conductivity data from 0–300 K are read from Holland's[16] measurements (the sample with impurity concentration 7×10^{15} cm^{-3} and characteristic cross-sectional dimension of 0.729 cm). For temperature above 300 K, Amith et al.[17] experimental data are adopted (the undoped n-type sample with impurity concentration 5.0×10^{16} cm^{-3}). According to Amith et al., the electron contribution to the thermal conductivity is negligible for the sample. But above 600 K there is a strong photon contribution to the thermal conductivity, which is not excluded in the calculation of the phonon MFP. The volumetric heat capacity of GaAs is obtained by multiplying its specific heat[18] with its density, 5.31 g/cm^3. A special average of the transverse and the longitudinal phonon velocity, $v = (2v_T^{-1} + v_L^{-1})^{-1} = 3.3 \times 10^5$ cm/s, is used for the average phonon velocity.[19]

It is clear from Fig. 2 that even at room temperature, the phonon MFP, ~200 Å, is of the same order or even larger than typical quantum well dimension, therefore, use of bulk thermal conductivity data for the active region is inappropriate.

Thermal Conductivity of Bulk GaAs

Most of the existing theory for the prediction of thermal conductivity starts from the phenomenological BTE.[8,20] Under the relaxation time approximation its steady-state form is

$$\mathbf{v}\cdot\mathbf{grad}T\,\frac{df_q}{dT} = \frac{f_q^0(\boldsymbol{\lambda}) - f_q}{\tau_n} + \frac{f_q^0 - f_q}{\tau_u} \tag{2}$$

where τ_n is the relaxation time for all normal processes—the ones that conserve momentum—mainly the three phonon normal process (N-process). τ_u is the relaxation time for those processes that do not conserve momentum including, e.g., the scattering due to impurity, defects, and the three phonon umklapp process (U-process). The toatl τ_u is obtained according to Matthiessen's rule by adding the reciprocal relaxation time for the appropriate processes. f_q^0 and $f_q^0(\boldsymbol{\lambda})$ are the Planck and the displaced Planck distributions which the U-process and the N-process approach at equilibrium, respectively.

Callaway[20] manipulated the above equation and obtained an expression for the thermal conductivity

$$k = CT^3 \int_0^{\theta_D/T} \frac{x^4 e^x (e^x - 1)^{-2}}{v_b/L + \alpha x^4 T^4 + (\beta_1 + \beta_2) x^2 T^5}\,dx + k_2 \tag{3}$$

Table 1 Parameters used in modeling the thermal conductivity of GaAs

$v \times 10^5$, cm/s[a]				Temperatures, K[b]								
v_T	v_L	v_{tu}	v_b	θ_1	θ_2	θ_3	θ_D	β_{tu}	β_t	β_L	α[c]	F[d]
2.48	5.24	1.05	3.3	99	113	326	345	0.91×10^5	6.5	0.264	1.36	0.75

[a] V_T, V_L, V_b from Holland,[16] V_{tu} the phonon group velocity at $\zeta = 0.5$ in Waugh and Dolling's phonon spectrum of GaAs in [100] direction.[22]
[b] θ_1, θ_2, θ_3 calculated using corresponding frequency in Waugh and Dolling's phonon spectrum of GaAs,[22] θ_D from Holland.[16]
[c,d] From Holland.[16]

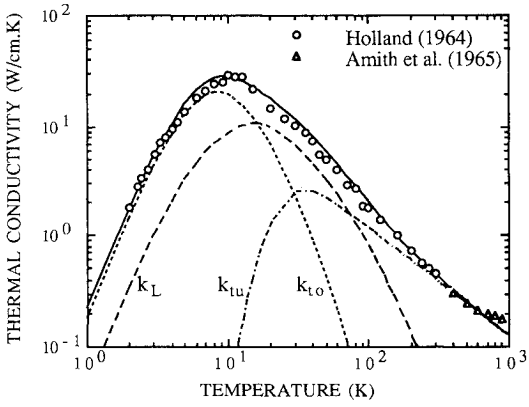

Fig. 3 Thermal conductivity of bulk GaAs.

where k_2 is a correction term due to the N-process and is generally neglected.[8] The denominator in the integrand is the sum of the inverse relaxation time of the individual scattering mechanisms according to Matthiessen's rule: the first term is due to boundary scattering; the second term represents the scattering by impurities and isotopes; and the third term includes the three phonon N- and U-processes.

Callaway's model has been successfully used in modeling the low temperature thermal conductivity of a wide range of semiconducting materials, including GaAs,[8,16] but it fails at high temperatures, e.g., above 100 K. Holland[19] extended Callaway's model and matched the thermal conductivity of silicon and germanium over 2–1000 K. His model emphasizes the difference of the longitudinal and the transverse phonon spectra of silicon and germanium.[21] For the transverse phonon branch, two phonon group velocities were used, one for the low frequency phonons ($\omega < \omega_1$) and the other for high frequency ones. According to Holland, the total thermal conductivity consists of three parts

$$k = k_{to} + k_{tu} + k_L \tag{4}$$

where k_L is longitudinal phonon contribution, k_{to} and k_{tu} are the contributions of low and high frequency transverse phonons, respectively. The various terms in Eq. (4) are given by

$$k_{to} = \frac{2}{3} T^3 \int_0^{\theta_1/T} \frac{C_{to} x^4 e^x (e^x - 1)^{-2}}{v_b/(FL) + \alpha x^4 T^4 + \beta_t x T^5} \, dx \tag{5}$$

$$k_{tu} = \frac{2}{3} T^3 \int_{\theta_1/T}^{\theta_2/T} \frac{C_{tu} x^4 e^x (e^x - 1)^{-2}}{v_b/(FL) + \alpha x^4 T^4 + \beta_{tu} x^2 T^2/\sinh x} \, dx \tag{6}$$

$$k_L = \frac{1}{3} T^3 \int_0^{\theta_3/T} \frac{C_L x^4 e^x (e^x - 1)^{-2}}{v_b/(FL) + \alpha x^4 T^4 + \beta_L x^2 T^5} \, dx \tag{7}$$

The denominators in the integrands of the above equations are similar to that in Eq. (3) except the three phonon processes are replaced by appropriate forms.

Due to the similarity of the phonon spectra among GaAs, Si, and Ge,[21,22] Holland's model should be applicable to GaAs. Following similar procedures used in Holland's paper, the thermal conductivity of GaAs is matched with the experimental data as shown in Fig. 3. Also shown in Fig. 3 are contributions from each of the three terms. Table 1 gives the coefficients used in the calculation. β_{tu} is obtained by matching the experimental data at 600 K, β_L is derived from data at 300 K, and β_t is extracted by matching the low temperature data. The model is not expected to match experimental data at temperatures greater than 600 K because above this temperature photons also contribute to the thermal conductivity.[17] Compared with the experiment data, it is seen that the model is very good at high and low temperatures. At intermediate temperatures between 10–100 K, the measured thermal conductivity is lower than the theoretical curve. This is due to the resonance scattering associated with impurities,[16] which is not included in the model.

Equation of Phonon Radiative Transfer

When the phonon MFP is of the same order or longer than the characteristic specimen dimension, boundary conditions will affect the phonon distributions inside the medium, and the energy transfer process becomes volumetric. Klitsner et al.[23] showed through Monte Carlo simulation that a temperature jump exists at the specimen boundaries, analogous to the temperature slip in a radiative transfer medium.[24] In this case, it is not the temperature gradient but the temperature of the boundaries that governs the heat flow. Consequently, the a priori assumption that a temperature gradient exists in the medium is not satisfied and the simplified BTE [Eq. (2)] does not hold. Majumdar[14] recently developed from the original BTE the EPRT

$$\mu \frac{dI_\omega}{d\zeta} = I_\omega + I_\omega^0[T(\zeta)] \tag{8}$$

Note that $\zeta (= z/\tau_i v)$ depends on temperature as well as frequency. The spectral phonon intensity I_ω is defined as

$$I_\omega = v f_q \hbar \omega D(\omega)/4\pi \tag{9}$$

I_ω is the flux of phonon energy per unit time, per unit area perpendicular to the direction of the phonon propagation, per unit solid angle in the direction of phonon propagation and per unit frequency interval around ω.

A nontrivial question is how to define the temperature in the film because temperature is a concept at thermal equilibrium. In bulk medium, local thermal equilibrium is reached within a region of the order of phonon MFP. In this case, the equilibrium phonon distribution is described by the Planck distribution f_q^0. When the phonon MFP is larger than the specimen dimension, such a local equilibrium state is no longer attainable. Phonons at each points are not at equilibrium with each other. For example, some may be at a temperature close to one boundary and the others to that of another boundary. Ziman[6] gave a definition of the temperature at z such that $f_q(z)$, averaged over an energy surface in q-space, gives just the same total number of particles of that energy as f_q^0. Such a definition, however, may yield multiple values of temperature at one location since total phonon number at different frequency may correspond a different temperature of the Planck distribution. The local temperature is thus defined here such that the total number of phonons (integrated over all energy and wavevector) in one location equals that of the total number of phonons obeying the Planck distribution at that tem-

perature. This definition agrees with Swartz and Pohl's[13] discussion for the case where no internal scattering exists.

Due to the similarity of EPRT with the equation of radiative transfer,[24] many results from radiative heat transfer can be applied to the conduction problem. Majumdar[14] has discussed the so-called "acoustically thin" and the "acoustically thick" limits in analogy to the "optically thin" and the "optically thick" limits and has showed that the EPRT approaches the conventional heat conduction problem in the acoustically thick limit.

Thermal Conductivity Perpendicular to Film

As was previously mentioned, most of the heat generated flows perpendicularly to the film in a quantum well. In this case, a one-dimensional treatment is appropriate, as shown in Fig. 1a. The two-flux model of radiative transfer[24] can be applied and the EPRT becomes

$$\mu \, dI_\omega^+/d\zeta = I_\omega^+ + I_\omega^0[T(\zeta)], \qquad (0 < \theta < \pi/2) \quad (10)$$

$$\mu \, dI_\omega^-/d\zeta = I_\omega^- + I_\omega^0[T(\zeta)], \qquad (\pi/2 < \theta < \pi) \quad (11)$$

It should be noted that the two-flux model is in essence the same as Fuchs and Sondheimer's model.[25] The difference lies in the use of the phonon radiation intensity instead of the distribution function.

Boundary Conditions

To solve Eqs. (10) and (11), boundary conditions at the two interfaces have to be specified. Phonon transmission and reflection at the interface of two solids has been a subject of study because of the thermal boundary resistance phenomena.[13] The most commonly accepted explanation is the acoustic mismatch theory, which attributes the temperature jump at the boundary to the difference of phonon propagation velocities in the two media. Besides the acoustic mismatch, other mechanisms, such as the boundary roughness,[26] are also responsible for the boundary thermal resistance. More recently, Swartz and Pohl[13] proposed a diffuse mismatch model in trying to obtain a better quantitative agreement with experimental data. The model assumes all the phonons are diffusely scattered at the interface. Ziman[6] gave a rough estimation of the fraction of specular phonon reflection at a surface as

$$p \approx \exp(-16\pi^3\eta^2/\lambda^2)$$

Under Debye approximation, the dominant phonon wavelength λ is about $2\pi v\hbar/\kappa T$. For the best interface, η is of the order of the lattice constant a. Substituting these quantities into the above equation, it is obtained that when

$$T > v\hbar/(2\sqrt{\pi}\kappa a)$$

the specular phonon reflection is less than e^{-1}. For GaAs, the above equation yields $T > 10$ K where v_T has been used for the phonon velocity, because from Fig. 2, k_{ω} dominates in such a temperature range. So for most temperatures, the phonon scattering can be considered as diffusive. Because of the simplicity of the diffuse mismatch model it will be used in the following treatment. The scattering mechanism inside the bounding media, e.g., $Ga_{1-x}Al_xAs$, also favors the use of the diffuse mismatch model. It has been shown[27] that the reduction of the thermal conductivity of the $Ga_{1-x}Al_xAs$ below GaAs and AlAs is due to the mass difference scattering. Similarly mass difference scattering is expected at the boundary when phonons propagate from one medium into the next.

The diffuse mismatch model was developed to explain the thermal boundary resistance. In the following treatment, however, it will be applied to establish the boundary conditions for EPRT. The possible temperature difference between the two media at the interface will not be considered.

Using the Debye approximation, Swartz and Pohl[13] give the transmission coefficient at the interface from medium i to its neighboring medium 3-i as

$$\alpha_i(\omega) = \sum_j v_{3-i,j}^{-2} \Big/ \sum_{i,j} v_{i,j}^{-2} \qquad (12)$$

Evaluation of the transmission coefficient from Eq. (12) requires longitudinal as well as transverse phonon velocities. Unfortunately, a detailed phonon spectrum of the AlAs could not be found, not to mention those of the $Ga_{1-x}Al_xAs$ alloy. To proceed, approximations have to be made. It is known that the Debye velocity is related to the Debye frequency through[28]

$$N = \omega_D^3 V/6\pi^2 v^3 \qquad (13)$$

For the $Ga_{1-x}Al_xAs$ alloy, a pseudocrystal model has been used to predict its thermal conductivity.[27] Because the lattices of the GaAs and the AlAs are closely matched, the former is 5.6535 Å and the latter is 5.62 Å, the lattice constant of the pseudocrystal can be taken as the average of the two, $a = 5.636$ Å.[29] Since there are four GaAs molecules in a unit cell, N is related to the volume of the crystal as $N = 4V/a^3$. Inserting these relations into Eq. (13) gives the relation between the phonon velocity and the Debye temperature as

$$v = \kappa\hbar^{-1}(24\pi^2)^{-1/3}\theta_D a \qquad (14)$$

Steigmeier[29] obtained a relation between the Debye temperature and the atomic mass of the crystal

$$\theta_D = 4.19 \times 10^{-8} G/(a^3 M)^{1/2} \qquad (15)$$

where $G = 0.949$ for AlAs and 0.936 for GaAs. Such a small difference is neglected in the subsequent treatment and G is taken as the average of the two for the $Ga_{1-x}Al_xAs$ alloy.

The atomic mass of $Ga_{1-x}Al_xAs$ can be calculated by averaging those of GaAs and AlAs

$$M = 72.37(1 - x) + 50.95x \qquad (16)$$

Equations (14–16) relate the phonon velocity of $Ga_{1-x}Al_xAs$ with the AlAs concentration x, but they do not distinguish the transverse and the longitudinal phonons. To be consistent, instead of the measured transverse and longitudinal phonon velocities, the same formulas are used to estimate the phonon velocity for GaAs when calculating the transmission coefficient. The phonon velocity of GaAs thus calculated is 4.11×10^5 cm/s, which is not far from the average phonon velocity, 3.3×10^5 cm/s. The final expression for the transmission coefficient is

$$\alpha(\omega) = \alpha = (1 - 0.296x)/(2 - 0.296x) \qquad (17)$$

Because of the Debye approximation, the transmission coefficient is independent of phonon frequency in the diffuse mismatch model. Also note that the maximum possible value of α is 0.5 in the diffuse mismatch model.[13]

With the transmission coefficient decided, the boundary conditions for the phonon intensity can be written as

$$I_\omega^+(0) = (1 - \alpha_1)I_\omega^-(0) + \alpha_1 I_\omega(T_1) \qquad (18)$$

$$I_\omega^-(\zeta_h) = \alpha_2 I_\omega(T_2) + (1 - \alpha_2)I_\omega^+(\zeta_h) \qquad (19)$$

In Eq. (18), the first term on the right side is the reflection of phonons at the boundary $\zeta = 0$ and the second term represents the transmission of phonon from the neighboring medium, which in its original form should be $\alpha_{3\to1} I_{\omega 3}(T_1)$, where $\alpha_{3\to1}$ is the transmission coefficient of phonons from the con-

fining medium into GaAs and $I_{\omega 3}$ is the phonon intensity in that medium. But according to the principle of detail balance,[13] it equals the last term in Eq. (18). Similar explanations hold for Eq. (19). These two boundary conditions are parallel to the ones used in radiation heat transfer,[24] with the transmission coefficient corresponding to the spectral emissivity.

Thermal Conductivity

Solving Eqs. (10) and (11) is straightforward.[24] The heat flux is obtained by integrating μI_ω over solid angle and frequency. When there is no internal source inside the medium—the case of phonon radiative equilibrium[14]—the derivative of the heat flux equals zero, which leads to an integral equation for the equilibrium phonon intensity distribution

$$\int_0^{\omega_D} \left\{ 2I_\omega^0[T(\zeta)] - I_\omega^+(0)E_2(\zeta) + I_\omega^-(\zeta_h)E_2(\zeta_h - \zeta) + \int_0^{\zeta_h} I_\omega^0 E_1(|\zeta - \zeta^*|)\, d\zeta \right\} \Big/ (\tau_i v)\, d\omega = 0 \quad (20)$$

where $E_n(z)$ is the exponential integral defined as[24]

$$E_n(z) = \int_0^1 \mu^{n-2} \exp(-z/\mu)\, d\mu$$

Only in a few special cases are analytical solutions of the above integral equation possible because of the strong dependence of τ_i on ω. A well-documented example in radiative heat transfer is the gray medium approximation,[24,30] which corresponds to a τ_i independent of frequency. In this case, the integral equation can be transformed to a standard form and its solution is a universal function. It is found that the radiative heat flux can be approximated very well by

$$\Psi = q/\{\pi[I_\omega^+(0) - I_\omega^-(\zeta_h)]\} = 1/(1 + 3\zeta_h/4) \quad (21)$$

For phonon radiative transfer, the gray medium approximation is difficult to justify. But since no other known simple solution exists, it is assumed here that Eq. (21) is a good approximation for the spectral heat flux. This corresponds to the solution of $dq_\omega/dz = 0$. It is not clear how rough this approximation is. The final "nice" expression for the thermal conductivity will show the tradeoff for such an approximation. Under this approximation and using Eqs. (18) and (19), the spectral phonon energy flux can be written as

$$q_\omega = \pi[I_\omega(T_1) - I_\omega(T_2)]/(\Psi_\omega^{-1} + \alpha_1^{-1} + \alpha_2^{-1} - 2) \quad (22)$$

where the subscript ω has been attached to Ψ to emphasis that it depends on frequency.

For small temperature differences the apparent thermal conductivity perpendicular to the active region can be obtained

$$k_z = \frac{-h}{\Delta T} \int_0^{\omega_D} q_\omega\, d\omega = \frac{\kappa^4 T^3}{2\pi^2 \hbar^3 v} \cdot \int_0^{\theta_D/T} \frac{x^4 e^x (e^x - 1)^{-2}}{\tau_i^{-1} + 4v(\alpha_1^{-1} + \alpha_2^{-1} - 1)/3h}\, dx \quad (23)$$

where the integral has been multiplied by a factor of three to account for the three phonon polarizations.

Equation (23) is similar to Callaway's model if the correction factor is taken as

$$F = 3/[4(\alpha_1^{-1} + \alpha_2^{-1} - 1)] \quad (24)$$

The denominator in the integrand of Eq. (23) is the inverse total relaxation time. It shows that at least under the approximations invoked above, Matthiessen's rule holds for the boundary scattering.

With F in Holland's model replaced by Eq. (24), the thermal conductivity perpendicular to the film is obtained. If the boundaries were black, $\alpha_1 = \alpha_2 = 1$, Eq. (24) gives $F = 0.75$, which coincides with what Holland used.[16] But this is only a coincidence because the factor F there corrects for the finite length of the specimen and depends on the length-to-width ratio. Also, as mentioned above, the transmission coefficient from the diffuse mismatch model excludes the case $\alpha_1 = \alpha_2 = 1$. The following calculation uses Holland's model except the boundary scattering term is considered separately, as in Eq. (23). Results for films thicker than the typical active region are also presented. Only symmetric QW, $\alpha_1 = \alpha_2 = \alpha$, are included.

Figure 4 shows that at low temperatures the thermal conductivity of GaAs in the QW can be several orders-of-magnitude smaller than that of its bulk value. This is because at these temperatures the internal scattering length is much greater than the well width. The shift of the maximum position reflects the fact that boundary scattering becomes effective at higher temperatures with decreasing film thickness. Similar trends are observed for polycrystalline diamond films.[31] Even at room temperature, the size effects exist for films of several microns. Also shown in Fig. 4 are the cases $\alpha_1 = \alpha_2 = 1$, the black boundaries, though they are excluded from the diffuse mismatch model. The influence of the boundary conditions is also illustrated in Fig. 5, which displays the change of thermal conductivity with film thickness at 300 K. Increasing the transmission coefficients (i.e., decreasing the AlAs concentration x in the boundary medium) will increase the thermal conductivity because a decreased transmission coefficient means more phonons are reflected back to the region, therefore, less heat leaves. This is different from the case of heat flow parallel to the film,[5] for which a higher specular reflection at the boundary means an increase in the phonon MFP and thus an increase in the thermal conductivity.

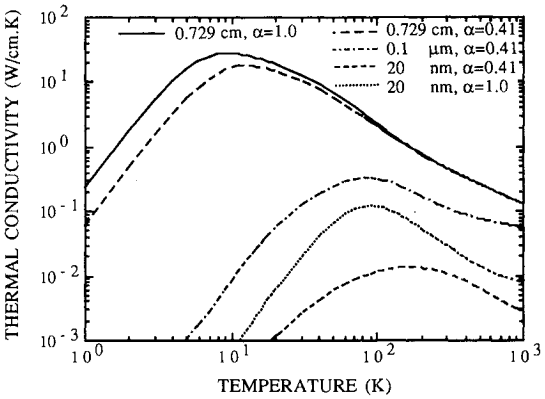

Fig. 4 Thermal conductivity perpendicular to the film vs temperature at different film thickness and boundary conditions.

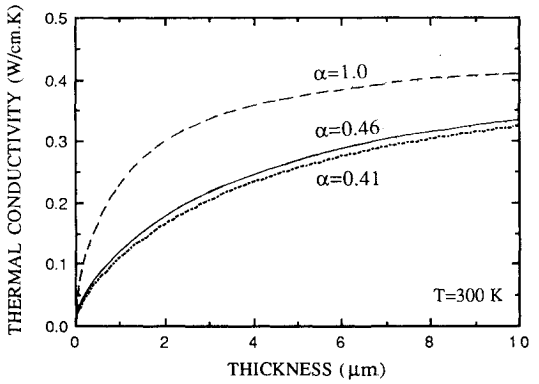

Fig. 5 Thermal conductivity perpendicular to the film vs film thickness.

But according to Fig. 2, the phonon MFP at 300 K is about 200 Å, so that it may be asked why films about microns still have size effects. The answer lies in the difference between Eqs. (1) and (3). In Eq. (1) the volumetric heat capacity includes both the transverse and the longitudinal phonon contributions; but from Fig. 3 it can be seen that at 300 K only the high frequency transverse phonons conduct heat effectively. A detailed investigation into the integral in Eq. (3) also reveals that in the integration interval (with increasing frequency) the total relaxation time decreases but the spectral phonon heat capacity increases, which means that the phonons with higher heat capacity do not carry heat proportionally. The net effect is also a reduction of the effective heat that the phonons can bring with them. Calculation of the specific heat using Debye's model showed good agreement with experiments, but the results corresponding to Holland's model are about four times smaller, which may indicate some flaws in Holland's model. From Table 1 typical relaxation time of the umklapp process at 300 K is about 10^{-9} s, corresponding to a relaxation length of a micron. This explains why films of micron thickness still exhibit size effects.

Another question one might ask is what happens if $x = 0$, which corresponds to a bulk GaAs. Two limiting cases may exist. One is that the active region is separated by irregular boundaries. This corresponds to grain boundaries in solids,[6] which will scatter phonons and the limit case is the diffuse scattering with $\alpha_1 = \alpha_2 = 0.5$. The other limit is a perfect crystal, in this case, a meaningful local temperature must be in a region of the order of the phonon MFP; arbitrarily taking a region of dimension smaller than the phonon MFP and using the formulation above will lead to unacceptable results.

It should be emphasized that the thermal conductivity obtained here is not an intrinsic property.[6,12] In fact, the above derivation clearly demonstrates that the Fourier diffusion equation does not hold. The temperature distribution should be obtained by solving the integral Eq. (20). Analogous to the radiative heat transfer, a temperature slip may occur at the boundary.[23,24] But such a slip is more fundamental and cannot be compensated through other modes of heat transfer.

Thermal Conductivity Parallel to Film

For quantum well structures and thin films on substrates, heat flows mainly perpendicular to the film. However, there is also heat flowing in the lateral direction. In this section the thermal conductivity parallel to the film will be discussed. For simplicity the following assumptions are made: 1) heat flows parallel to the film; 2) the lateral lengths are much larger than both the film thickness and the phonon MFP so that the film can be considered as infinitely long and wide; 3) diffuse boundary scattering; and 4) the temperature is uniform in the cross section.

The following analysis is similar to Herring,[7] but the EPRT is used. In two dimensions, as shown in Fig. 1b, EPRT can be written as

$$v_y \frac{dI_\omega^0}{dT}\frac{dT}{dy} + v_z \frac{dI_\omega}{dz} = \frac{I_\omega^0[T(y)] - I_\omega}{\tau_i(\omega)} \tag{25}$$

The first term in the above equation is an approximation of dI_ω/dy. Because of assumption 2), a temperature gradient exists along the y direction. The second term on the right reflects the effects of the boundary.

Since the first term on the left does not change with z, the two-flux model can be applied for the z direction. The solutions are

$$I_\omega^+(\zeta) = I_\omega^+(0)\exp\left(\frac{-\zeta}{\mu}\right) + (\tau_i R_y + I_\omega^0) \cdot \left[1 - \exp\left(\frac{-\zeta}{\mu}\right)\right] \tag{26}$$

$$I_\omega^-(\zeta) = I_\omega^-(\zeta_h)\exp\left(\frac{\zeta_h - \zeta}{\mu}\right) - (\tau_i R_y + I_\omega^0) \cdot \left[\exp\left(\frac{\zeta_h - \zeta}{\mu}\right) - 1\right] \tag{27}$$

where

$$R_y = -v_y(dI_\omega^0/dT)(dT/dy) = -\sin\theta\cos\varphi R \tag{28}$$

The heat flux in the y direction is

$$q = \frac{1}{h}\int_0^h dz \int_0^{\omega_D} d\omega \int_{4\pi} I_\omega \sin\theta\cos\varphi\, d\Omega \tag{29}$$

Substituting Eqs. (26) and (27) into Eq. (29), and performing the integration yields the thermal conductivity parallel to the film as

$$k_y = \frac{\kappa^4}{2\pi\hbar^3 v}\int_0^{\theta_D/T} \tau_t(1 - 3g/2)x^4 e^x(e^x - 1)^{-2}\, dx \tag{30}$$

where a factor of three has been included to account for the three phonon polarizations. The universal function g is related to the exponential function E_n[24] as

$$g = \{1 - 4[E_3(\zeta_h) - E_5(\zeta_h)]\}/\zeta_h \tag{31}$$

Equation (30) is identical to Callaway's model if the total relaxation time in Eq. (3) is replaced by

$$\tau_t = \tau_i(1 - 3g/2) \tag{32}$$

To be consistent in form with Matthiessen's rule, the boundary relaxation time can be defined as

$$\tau_b = \tau_i[2/(3g) - 1] \tag{33}$$

Such a definition, however, is of little use since it depends upon τ_i.

Two limiting cases of Eq. (30) can be obtained. When h is infinite, that is for a large specimen, g goes to zero, and k_y is identical to the expression for a bulk medium. When h is very small, by series expansion of the exponential functions,[24] g can be expressed as

$$g = -\tfrac{2}{3} + (-\gamma + 1 - \tfrac{1}{4}\zeta_h)\zeta_h \tag{34}$$

Substituting Eq. (34) into Eq. (32) gives

$$\tau_t = (-\gamma + 1 - \tfrac{1}{4}\zeta_h)h/3v \tag{35}$$

The above expression is analogous to Casimir's limit if the third term in the bracket is neglected. But this term is actually greater than the first two terms. In fact, according to Casimir's theory, the phonon MFP would diverge for parallel plates. Equation (35) gives a finite value, which is more reasonable.

To calculate the thermal conductivity parallel to the film, the total relaxation time in Holland's model is replaced by Eq. (32). Again, the internal scattering times are taken the same as in Eqs. (3–6) with the boundary terms moved. As in Holland's paper,[19] the average phonon velocity is used in ζ_h when calculating the factor g.

Figure 6 displays the thermal conductivity of GaAs parallel to the film. Note that it is independent of the transmission coefficient because of the diffuse boundary assumption. Dots in the figure are thermal conductivities for an isolated specimen of square cross section of length 0.729 cm calculated from Holland's original model. At high temperatures, they approach those of a film of 0.729-cm thickness. But at low temperatures they are smaller than those of the film because phonons in the film are not confined in the lateral directions

and, therefore, have higher MFP. Figure 7 gives the variation of thermal conductivity with film thickness at two temperatures. Again, the size effects are more important at low temperatures, and at room temperature films of micron thickness still show size effects.

Even though the unit cell of the film is cubic, there is an anisotropy in thermal conductivity due to the size effects.[12] The ratio of k_z to k_y is plotted in Fig. 8. Thermal conductivity in the direction parallel to the film is larger than that perpendicular to it because phonons parallel to the film have longer MFP than those perpendicular to it.

Some limitations of the current model are discussed here. This work considers single crystal films. No effects of columnar structure and cracks are included. If these effects can be treated as volumetric and homogeneous, however, they can be included in the internal relaxation time and the model still applies. The effects of doping can be taken into account by adjusting the impurity scattering parameter α. The directional dependence of phonon group velocity is not included. The latter may cause phonon focusing.[32] Holland's model is applied because of the similarity of phonon spectra among GaAs, Si, and Ge, but the formulas developed for treating the boundary and the size effects are more general. The success of the model depends on the accuracy of the internal scattering time. Finally, the possible change of the density of states due to the near two-dimensionality is not considered. If this were included, the specific heat as well as the functional forms of various relaxation time should be revised.

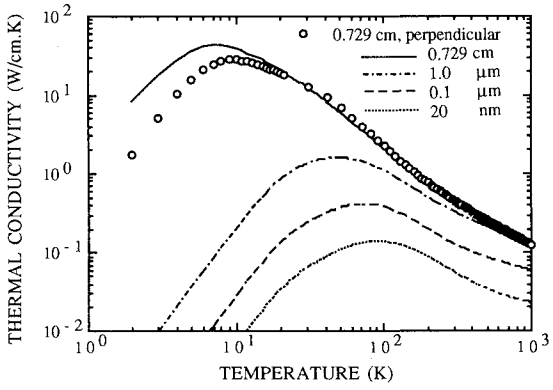

Fig. 6 Thermal conductivity parallel to the film vs temperature at different film thickness.

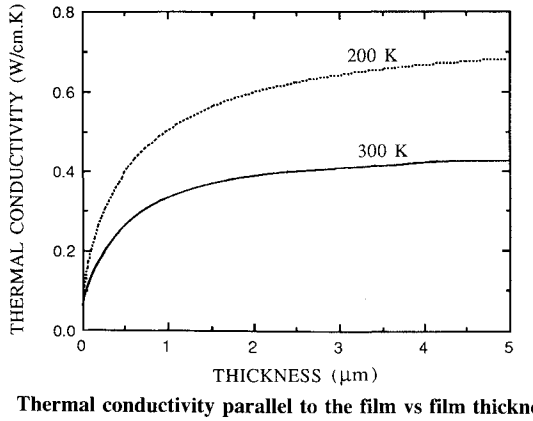

Fig. 7 Thermal conductivity parallel to the film vs film thickness.

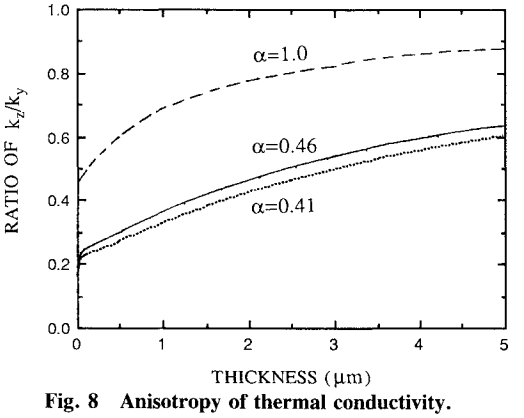

Fig. 8 Anisotropy of thermal conductivity.

Conclusions

Thermal conductivity is an important property in the design of QW structures. Due to the extremely small dimension of the common QW, the boundary and size effects are important even at room temperatures. This article presents a theoretical study of the size effects on the thermal conductivity of the active region in a quantum well.

Holland's model is applied for the thermal conductivity of bulk GaAs, the most commonly used semiconducting QW material. The model matches the experimental data from 2–600 K satisfactorily.

When the phonon MFP in a specimen is of the same order as the typical dimension of the active region, the commonly used temperature gradient assumption is not valid. The equation of EPRT developed from the BTE[14] is applied in predicting the thermal conductivity of GaAs in a QW. Boundary conditions for the EPRT are established from the diffuse phonon mismatch model.[13] Thermal conductivity in the direction perpendicular to the film is then obtained under certain approximation. The calculation shows that the film thickness has very strong effects on the thermal conductivity. The boundary conditions (e.g., the concentration of AlAs in the bounding media), also affect the thermal conductivity of the active region. Thermal conductivity parallel to the film is quantified. Due to the diffuse boundary assumption, the boundary media have no effect on the thermal conductivity in this direction. For both cases, the size effects exist at room temperature for films with thickness on the order of microns. Anisotropy of thermal conductivity caused by the size and boundary effects is discussed.

Acknowledgments

The authors gratefully acknowledge the financial support from the U.S. Department of Energy, and the K. C. Wong Education Foundation. They also thank A. Majumdar of Arizona State University for permitting them to use his results before publishing and his comments, and M. I. Flik's group in MIT for their comments.

References

[1]Yariv, A., *Quantum Electronics*, 3rd ed., Wiley, New York, 1989, pp. 264–276.

[2]Joyce, W. B., and Dixon, R. W., "Thermal Resistance of Heterostructure Lasers," *Journal of Applied Physics*, Vol. 46, No. 2, 1975, pp. 855–862.

[3]De Haas, W. J., and Biermasz, Th., "The Dependence on Thickness of the Thermal Resistance of Crystals at Low Temperatures," *Physica*, Vol. 5, No. 7, 1938, pp. 619–624.

[4]Casimir, H. B. G., "Note on the Conduction of Heat in Crystals," *Physica*, Vol. 5, No. 6, 1938, pp. 495–500.

[5]Berman, R., Foster, E. L., and Ziman, J. M., "Thermal Conduction in Artificial Sapphire Crystals at Low Temperatures," *Proceedings of the Royal Society A* (London), Vol. 231, No. 1184, 1955, pp. 130–144.

[6]Ziman, J. M., *Electrons and Phonons*, Clarendon Press, Oxford, England, UK, 1960, Chaps. 1, 8, and 11.

[7]Herring, C., "Theory of Thermoelectric Power of Semiconductors," *Physical Review*, Vol. 96, No. 5, 1954, pp. 1163–1187.

[8]Carruthers, P., "Theory of Thermal Conductivity of Solids at Low Temperatures," *Reviews of Modern Physics*, Vol. 33, No. 1, 1961, pp. 92–138.

[9]Lambropoulos, J. C., "Thermal Conductivity of Dielectric Thin Films," *Journal of Applied Physics*, Vol. 66, No. 9, 1989, pp. 4230–4242.

[10]Redondo, A., and Beery, J. G., "Thermal Conductivity of Optical Coatings," *Journal of Applied Physics*, Vol. 60, No. 11, 1986, pp. 3882–3995.

[11]Volklein, F., and Kessler, E., "Analysis of the Lattice Thermal Conductivity of Thin Films by Means of a Modified Mayadas-Shatzkes Model: The Case of Bismuth Films," *Thin Solid Films*, Vol. 142, No. 2, 1986, pp. 169–181.

[12]Flik, M. I., and Tien, C. L., "Size Effect on the Thermal Conductivity of High-Tc Thin Film Superconductors," *Journal of Heat Transfer*, Vol. 112, Nov. 1990, pp. 872–881.

[13]Swartz, E. T., and Pohl, R. O., "Thermal Boundary Resistance," *Review of Modern Physics*, Vol. 61, No. 3, 1989, pp. 605–668.

[14]Majumdar, A., "Microscale Heat Conduction in Dielectric Thin Films," ASME HTD, Vol. 184, Atlanta, GA, 1991, pp. 34–41.

[15]Tien, C. L., and Lienhard, J. H., *Statistical Thermodynamics*, Hemisphere, New York, 1979, Chap. 11.

[16]Holland, M. G., "Phonon Scattering in Semiconductors from Thermal Conductivity Studies," *Physical Review*, Vol. 134, No. 2A, 1964, pp. A471–A480.

[17]Amith, A., Kudman, I., and Steigmeier, E. F., "Electron and Phonon Scattering in GaAs at High Temperatures," *Physical Review*, Vol. 138, No. 4A, 1965, pp. A1270–A1276.

[18]Touloukian, Y. S., Powell, R. W., Ho, C. Y., and Klemens, P. G., "Thermal Physics Properties of Matter," *TPRC Data Series*, Vol. 5, IFI/Plenum Press, New York, 1970, pp. 307–309.

[19]Holland, M. G., "Analysis of Lattice Thermal Conductivity," *Physical Review*, Vol. 132, No. 6, 1963, pp. 2461–2471.

[20]Callaway, J., "Model for Lattice Thermal Conductivity at Low Temperatures," *Physical Review*, Vol. 113, No. 4, 1959, pp. 1046–1051.

[21]Brockhouse, B. N., "Lattice Vibrations in Silicon and Germanium," *Physical Review Letters*, Vol. 2, No. 6, 1959, pp. 256, 257.

[22]Waugh, J. L. T., and Dolling, G., "Crystal Dynamics of Gallium Arsenide," *Physical Review*, Vol. 132, No. 6, 1963, pp. 2410–2412.

[23]Klitsner, T., VanCleve, J. E., Fischer, H. E., and Pohl, R. O., "Phonon Radiative Heat Transfer and Surface Scattering," *Physical Review B*, Vol. 38, No. 11, 1988, pp. 7576–7594.

[24]Siegel, R., and Howell, J. R., *Thermal Radiation Heat Transfer*, McGraw-Hill, New York, 1981, Chaps. 14 and 15.

[25]Tellier, C. R., and Tosser, A. J., *Size Effects in Thin Films*, Elsevier, Amsterdam, 1982, Chap. 1.

[26]Majumdar, A., "Effect of Interfacial Roughness on Phonon Radiative Heat Conduction," *Journal of Heat Transfer*, Vol. 113, Nov. 1991, pp. 797–805.

[27]Afromowitz, M. A., "Thermal Conductivity of $Ga_{1-x}Al_xAs$ Alloys," *Journal of Applied Physics*, Vol. 44, No. 3, 1973, pp. 1292–1294.

[28]Kittel, *Introduction to Solid State Physics*, Wiley, New York, 1986, Chap. 5.

[29]Steigmeier, E. F., "The Debye Temperature of III-V Compounds," *Applied Physics Letters*, Vol. 3, No. 1, 1963, pp. 6–8.

[30]Heaslet, M. A., and Warming, R. F., "Radiative Transport and Wall Temperature Slip in an Absorbing Planar Medium," *International Journal of Heat and Mass Transfer*, Vol. 8, No. 7, 1965, pp. 979–994.

[31]Morelli, D. T., Beetz, C. P., and Perry, T. A., "Thermal Conductivity of Synthetic Diamond Films," *Journal of Applied Physics*, Vol. 64, No. 6, 1988, pp. 3063–3066.

[32]Blakemore, J. S., "Semiconducting and Other Major Properties of Gallium Arsenide," *Journal of Applied Physics*, Vol. 53, No. 10, 1982, pp. R123–R181.